Supporting information

Effect of Manganese Promotion on the Activity and Selectivity of Cobalt Catalysts for CO Preferential Oxidation

Liping Zhong,[a], Mathias Barreau,[a,*] Dingkai Chen,[a] Valérie Caps,[a] Michael Haevecker,[b,c] Detre Teschner, [b,c c] David H. Simonne,[d] Elisa Borfecchia,[d] Walid Baaziz,[e] Břetislav Šmíd,[f] and Spyridon Zafeiratos,[a,*]

[a]*Institut de Chimie et Procédés pour l'Energie, l'Environnement et la Santé (ICPEES), ECPM, UMR 7515 CNRS – Université de Strasbourg, 25 rue Becquerel, 67087 Strasbourg Cedex 02, France*

[b]*Max-Planck-Institut für Chemische Energiekonversion (MPI-CEC), Stiftstrasse 34-36, D-45470 Mülheim a.d. Ruhr, Germany*

[c]*Fritz-Haber-Institut der Max-Planck-Gesellschaft, Faradayweg 4-6, D-14195 Berlin, Germany*

[d]*Department of Chemistry, INSTM Reference Center and NIS Centers, University of Torino, Via P. Giuria 7, 10125 Torino, Italy*

[e]*Institut de Physique et Chimie des Matériaux de Strasbourg (IPCMS), UMR 7504 CNRS – Université de Strasbourg, 23 rue du Loess BP 43, 67034 Strasbourg cedex 2, France*

[f]*Charles University, Faculty of Mathematics and Physics, Department of Surface and Plasma Science, V Holešovičkách 2, 18000, Prague 8, Czech Republic*

* *mbarreau@unistra.fr*

**spiros.zafeiratos@unistra.fr*

Supporting information 1: Calculation of conversion and selectivity based on mass spectrometry data in NAP-XPS cell with AlKα X-ray source

The CO and O_2 conversion, as well as the CO_2 and CH_4 selectivity of the 3 catalysts during the *operando* NAP-XPS tests performed at Charles University in Prague, were calculated by the quadruple mass spectrometer signal (QMS) *on line* connected to the NAP-XPS cell. Four QMS signals (i.e. m/e) were used for this purpose: CO (m/e=28), O_2 (m/e=32), CO_2 (m/e = 44) and CH_4 (m/e = 15). A correction of the ion current of m/e = 28 due to CO_2 fragment (11% of m/e = 44) was taken into account. In case of CH_4 the m/e = 15 (85% of m/e=16) was selected instead of m/e = 16 in order to avoid the influence of fragments from O_2 and CO_2. A typical evolution of QMS signal of the four masses as a function of time in the light-off catalytic tests is shown in Figure S1.

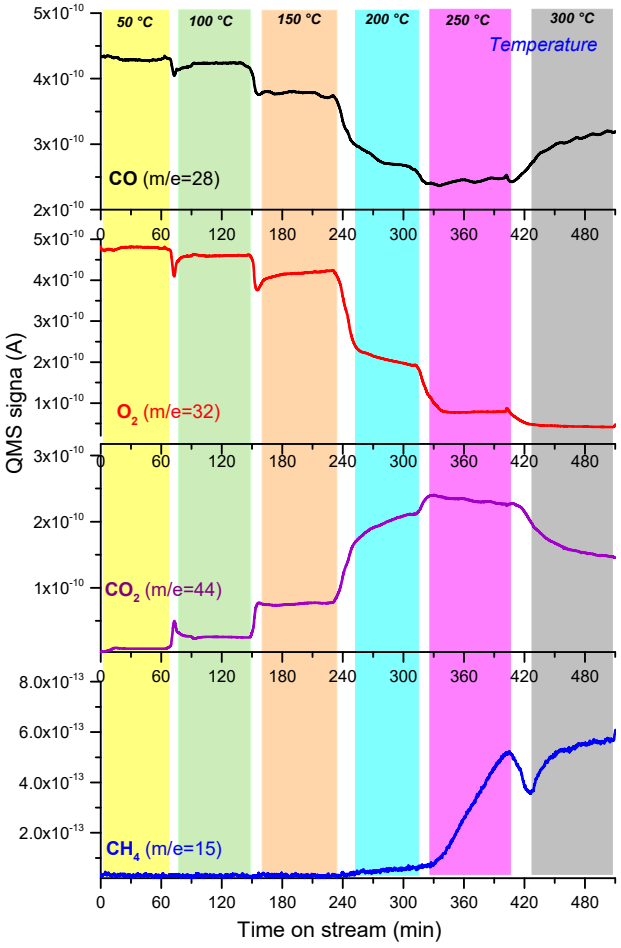

Figure S 1. On-line quadrupole mass spectrometry data recorded in the NAP-XPS cell upon heating the Co_8MnO_x catalyst in 1 mbar of 1% CO, 1% O_2 and 98% H_2, mixture. The vertical colored zones represent different reaction temperatures.

The decrease of CO and O_2 QMS signals under reaction conditions as compared to the signal at 50°C was used to calculate CO and O_2 conversions, X_{CO} and X_{O2} respectively, according to the equations:

$$X_{CO,T}\ (\%) = \frac{QMS_{CO,30°C} - QMS_{CO,T}}{QMS_{CO,30°C}} \times 100 \qquad \text{(Eq. S1)}$$

$$X_{O2,T}\ (\%) = \frac{QMS_{O2,30°C} - QMS_{O2,T}}{QMS_{O2,30°C}} \times 100 \qquad \text{(Eq. S2)}$$

The CO_2 and CH_4 product selectivities were calculated by the increase of the CO_2 (m/e = 44) and CH_4 (m/e = 15) QMS signals induced by the catalytic reaction according to the equations:

$$S_{CO2,T}\ (\%) = \frac{X_{CO,T}}{2X_{O2,T}} \times 100 \qquad \text{(Eq. S3)}$$

$$rel.S_{CH4,T} = \frac{Y_{CH4,T}}{X_{CO,T}} \qquad \text{where:} \quad Y_{CH4,T} = \frac{QMS_{CH4,T} - QMS_{CH4,30°C}}{QMS_{CH4,30°C}} \qquad \text{(Eq. S4)}$$

Where $QMS_{i,T}$ is the QMS signal of gas ι at reaction temperature T.

It should be noted that the QMS signals were not calibrated to the sensitivity factor of each gas. Therefore are used as a basis to compare the selectivity between different catalysts and temperatures (relative selectivity) assuming that the QMS signal and the mass concentration follow a linear relation. Note that the pressure in the mass spectrometer was proportional to the one in the NAP-XPS reaction cell and practically stable within the COPrOx experiment.

Supporting information 2: Comparison of Mn 2p spectra

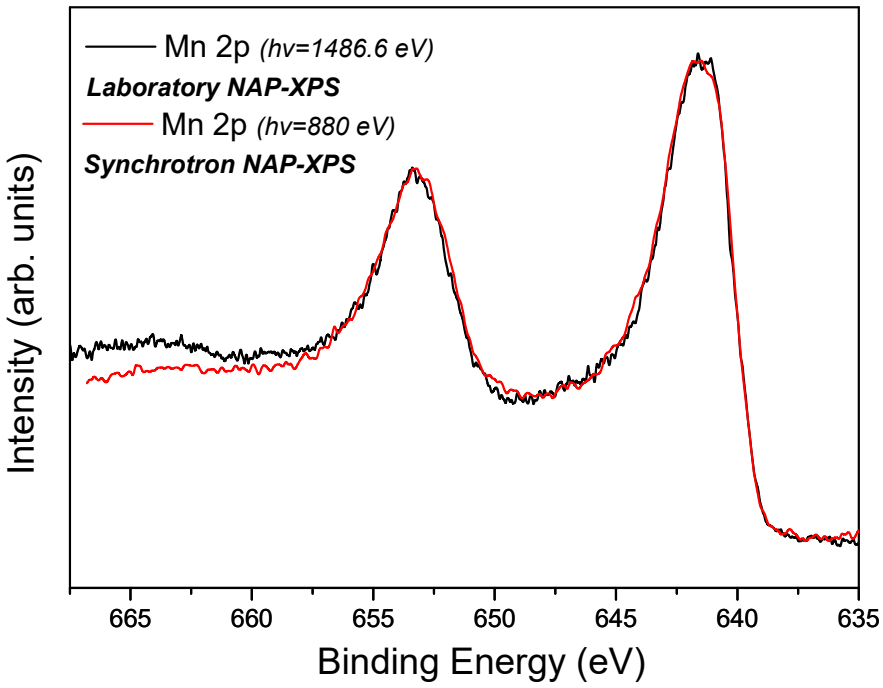

Figure S 2. Comparison of NAP-XPS Mn 2p spectra recorded over Co_8MnO_x catalysts using synchrotron radiation (hv=880 eV) and a laboratory monochromatic AlKα X-ray source (hv=1486.6 eV). The two Mn 2p peak have almost identical peak profiles. Please note that the intensity of the two spectra is normalized in order to compare their peak shape. In reality the spectrum of the synchrotron-based instrument has 35 times higher intensity than the laboratory source under the conditions employed for the two measurements.

Supporting information 3: XRD

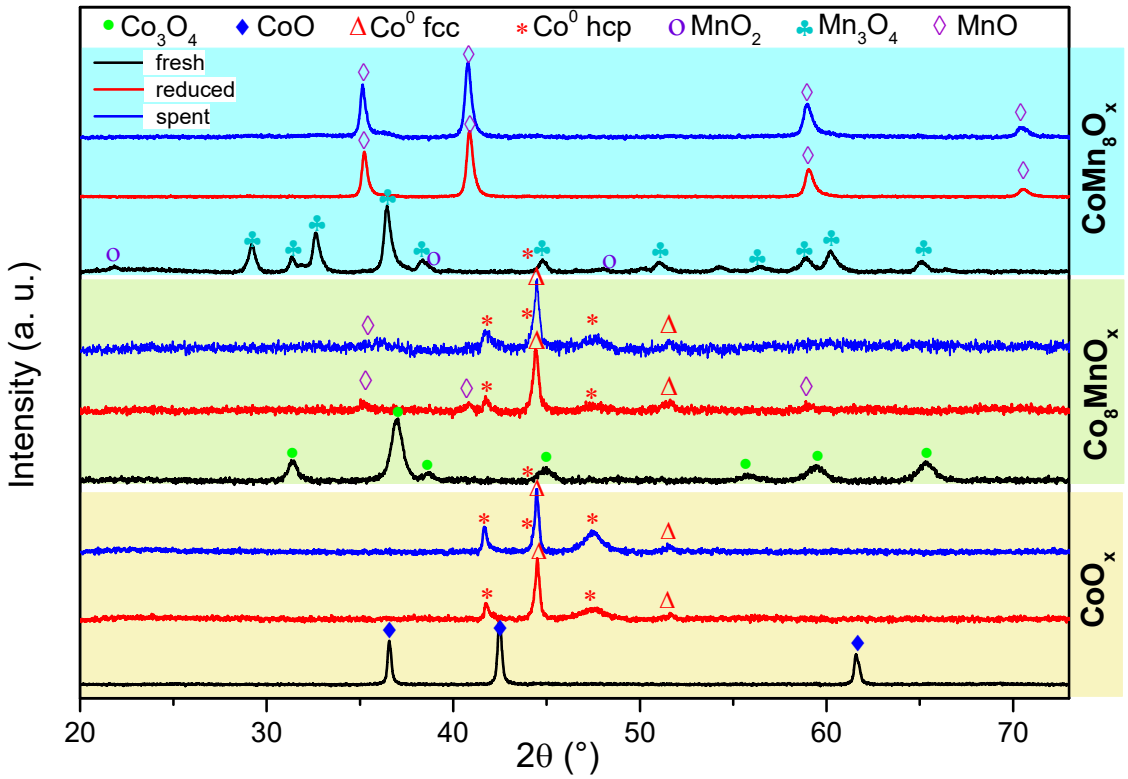

Figure S 3. XRD patterns of the fresh (after calcination), reduced in H_2 and spent CoO_x, Co_8MnO_x and $CoMn_8O_x$ catalysts.

.

Supporting information 4: H_2-TPR

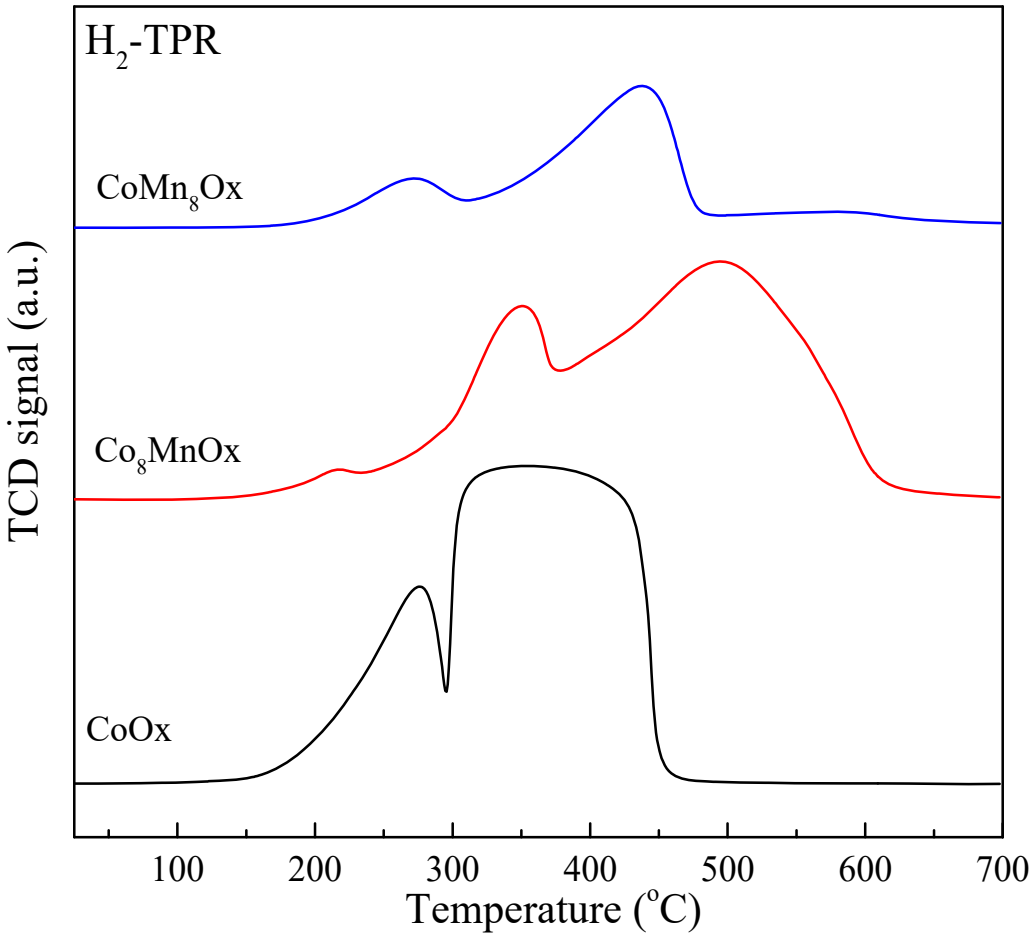

Figure S 4. H_2-TPR profiles of calcined pure CoOx (—), Co_8MnO_x (—) and$CoMn_8O_x$ (—).

Supporting information 5: SEM-EDX analysis

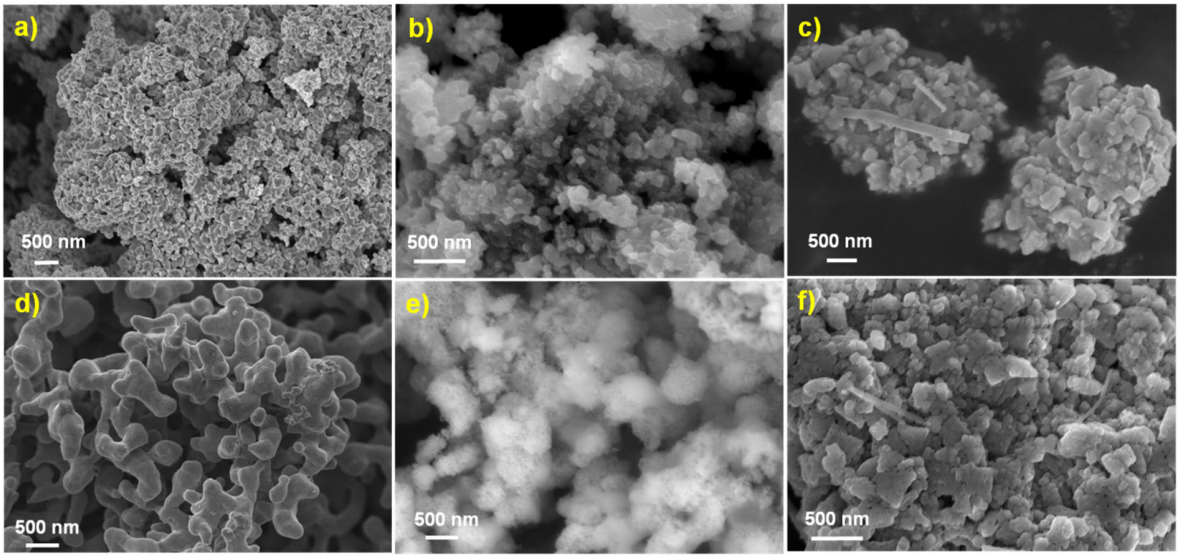

Figure S 5. SEM micrographs of the fresh a) CoO_x, b) Co_8MnO_x, c) $CoMn_8O_x$ and reduced d) CoO_x, e) Co_8MnO_x, f) $CoMn_8O_x$ catalysts.

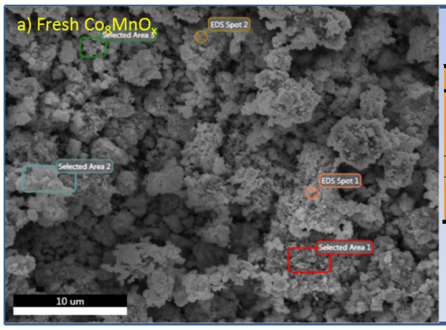

Fresh Co_8MnO_x

Atomic (%)	Area 1	Area 2	Area 3	Spot 1	Spot 2
O	29.7	53.6	13.8	56.8	56.7
Mn	6.5	4.6	7.7	3.4	3.3
Co	63.8	41.9	78.5	40.0	40.0
Atomic ratio					
Mn/Co	0.10	0.11	0.10	0.08	0.08
O/(Mn+Co)	0.42	1.15	0.16	1.30	1.31

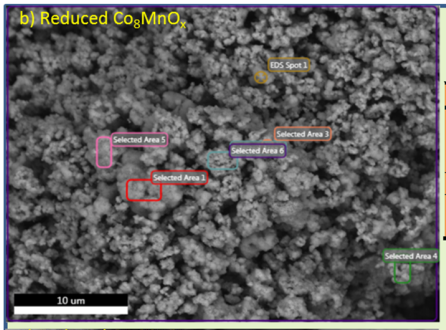

Reduced Co_8MnO_x

Atomic (%)	Area 1	Area 2	Area 3	Area 4	Area 5	Area 6	Spot 1
O	21.8	13.0	14.8	9.6	9.7	10.5	27.1
Mn	7.7	9.5	7.6	10.6	6.8	11.5	9.1
Co	70.5	77.5	77.7	79.7	83.6	78.0	63.8
Atomic ratio							
Mn/Co	0.11	0.12	0.10	0.13	0.08	0.15	0.14
O/(Mn+Co)	0.28	0.15	0.17	0.11	0.11	0.12	0.37

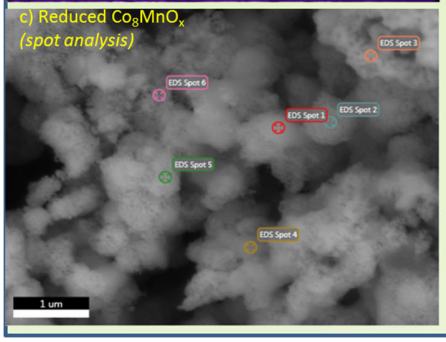

Reduced Co_8MnO_x (spot analysis)

Atomic (%)	Spot 1	Spot 2	Spot 3	Spot 4	Spot 5	Spot 6
O	40.8	14.0	12.6	34.5	24.6	26.9
Mn	24.5	8.8	10.1	21.1	8.4	7.8
Co	34.8	77.2	77.3	44.4	67.0	65.3
Atomic ratio						
Mn/Co	0.70	0.11	0.13	0.47	0.13	0.12
O/(Mn+Co)	0.69	0.16	0.14	0.53	0.33	0.37

Figure S 6. EDX analysis of several spots and areas of the surface of (a) fresh and (b,c) reduced Co_8MnO_x

Supporting information 6: STEM-EDX

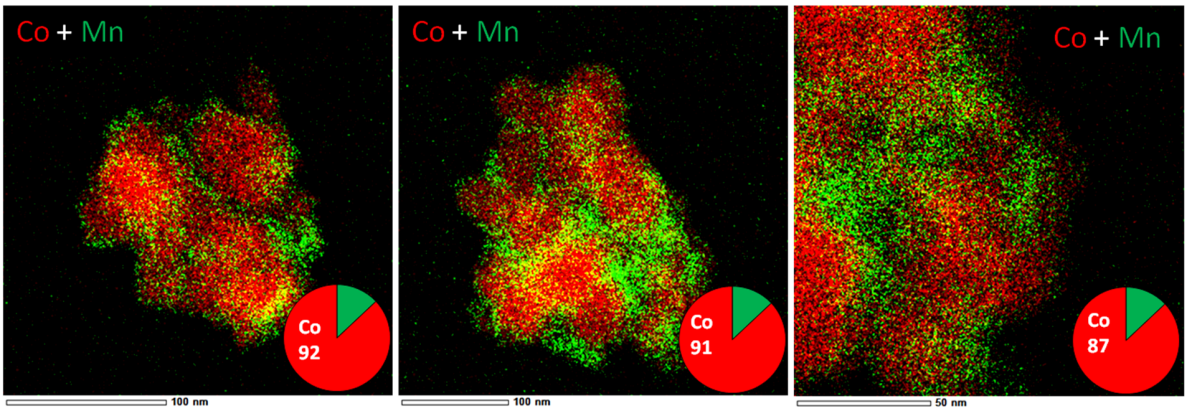

Figure S 7. STEM-EDX analysis images with elemental mapping (merged Co+Mn) collected over a fresh $CoMn_8O_x$ catalyst after calcination in air for 3 h at 400 °C. Red and green colored areas correspond to Co- and Mn-enriched areas, respectively. The % atomic concentration of Mn and Co is presented in the pie charts at the right-bottom side of each panel.

Supporting information 7: Short-term stability tests

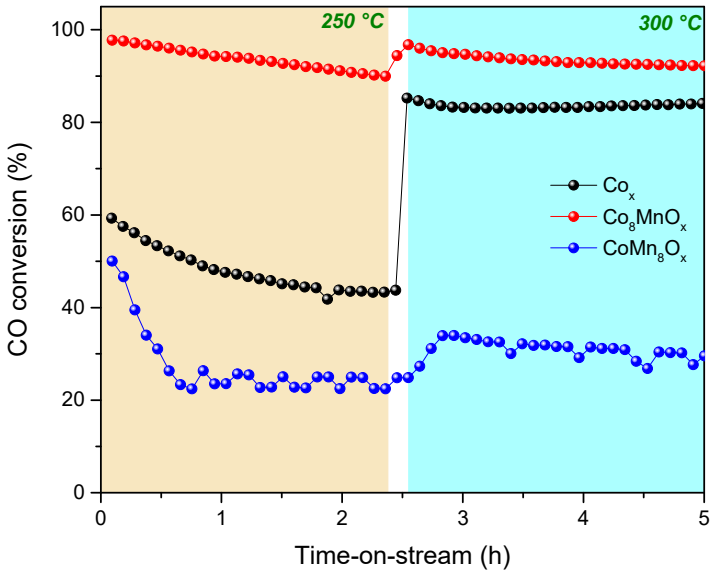

Figure S 8. CO conversion as a function of the time-on-stream at two characteristic temperatures for pure CoO_x (●), Co_8MnO_x (●) and $CoMn_8O_x$ (●) catalysts. *Experimental conditions*: 1% CO, 1% O_2, and 50% H_2 in He-balanced flow; 0.05 g of catalyst; 50 mL min^{-1} of total flow; atmospheric pressure (1 bar).

Table S1. Drop of the CO conversion of the two catalysts derived from the short-term stability tests shown in Figure S9.

Catalyst	Drop of X_{CO} per h on stream (%)	
	250 °C	***300 °C***
CoO_x	10	0
Co_8MnO_x	4	2
$CoMn_8O_x$	22	5

Supporting information 8: NAP-XPS depth profile measurements

Table S2. Measurements conditions of Co 2p and Mn 2p spectra used for the depth dependent NAP-XPS measurements and at.% Mn calculated for two information depths based on these spectra.

Photon energy (eV)	**Spectrum recorded**	**Photo-e kinetic energy** (eV)	**IMFP**[a] (nm)	**Information depth** (nm)[b]	**at.% Mn** (250 °C 55 min)	**at.% Mn** (350 °C 25 min)	**at.% Mn** (350 °C 55 min)
1340	Co 2p	550	1.23 (*for Co_3O_4*)	3.7	20.0	37.5	36.7
1200	Mn 2p	550	1.33 (*for Mn_2O_3*)	4.0			
1020	Co 2p	230	0.71	2.1	22.0	44.5	40.0
880	Mn 2p	230	0.77	2.3			

a. IMFP refers to the Inelastic Mean Free Path and its calculation was done by using the QUASES-IMFP-TPP2M software.

b. Calculated as 3 times of the IMFP

Supporting information 9: Examples of linear combination fit analysis applied on Co L_3-edge and Mn L_3-edge NEXAFS spectra recorded at 1 bar.

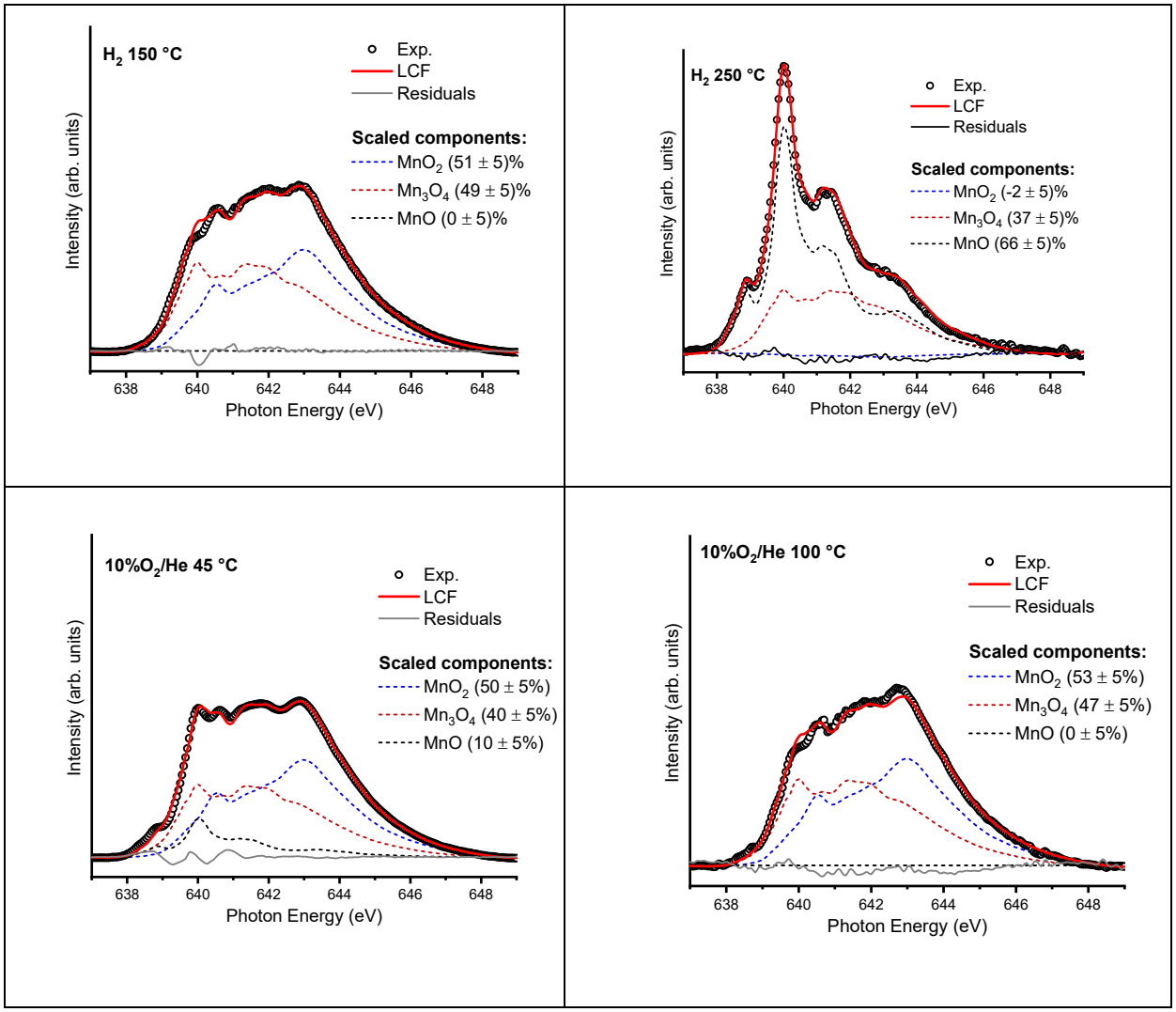

Figure S 9. Characteristic examples of liner combination fit analysis applied to the Co L_3-edge and Mn L_3-edge NEXAFS spectra in order to quantify the evolution of the various oxidation states during the redox treatment.

Supporting information 10: Mn $2p_{3/2}$ spectra from laboratory based NAP-XPS experiments

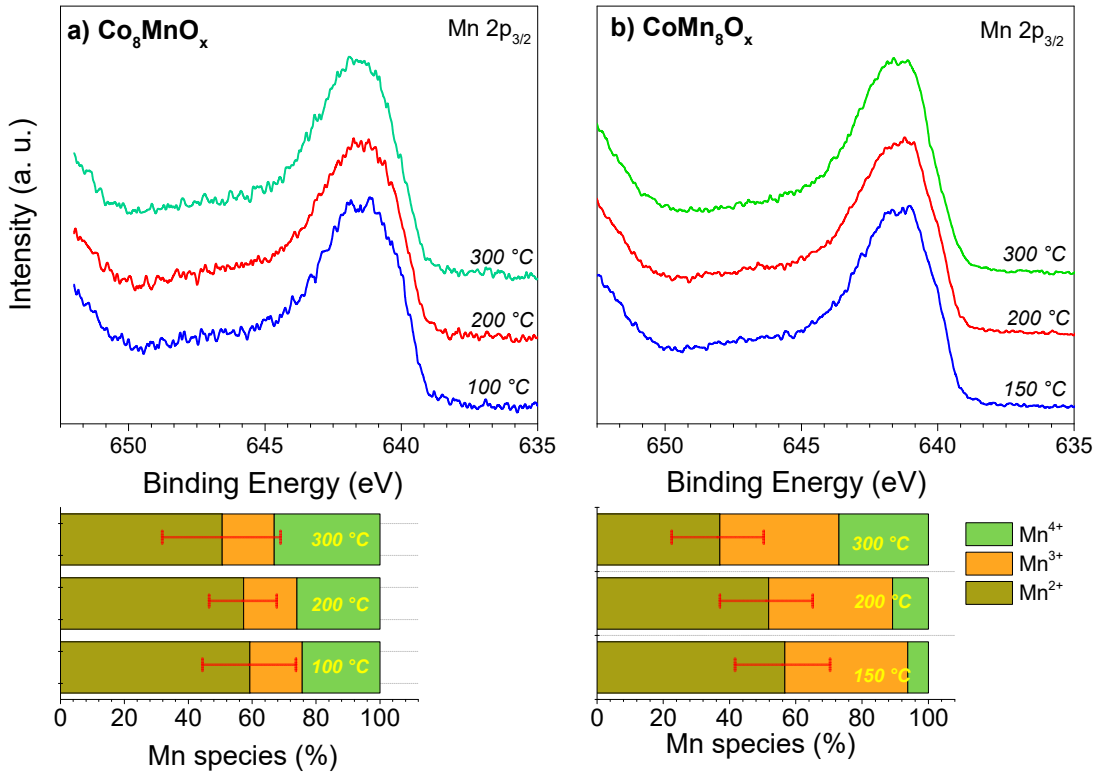

Figure S 10. In situ NAP-XPS spectra of Mn $2p_{3/2}$ on (a) Co_8MnO_x and (b) $CoMn_8Ox$ recorded after H_2 pretreatment during COPrOx at various temperatures. Distribution of manganese species resulting from Mn $2p_{3/2}$ deconvolution. Operating conditions: 1 mbar of 1% CO, 1% O_2 and 98% H_2, from room temperature to 300 °C.

Supporting information 11: HRSTEM of spent $CoMn_8O_x$ catalyst

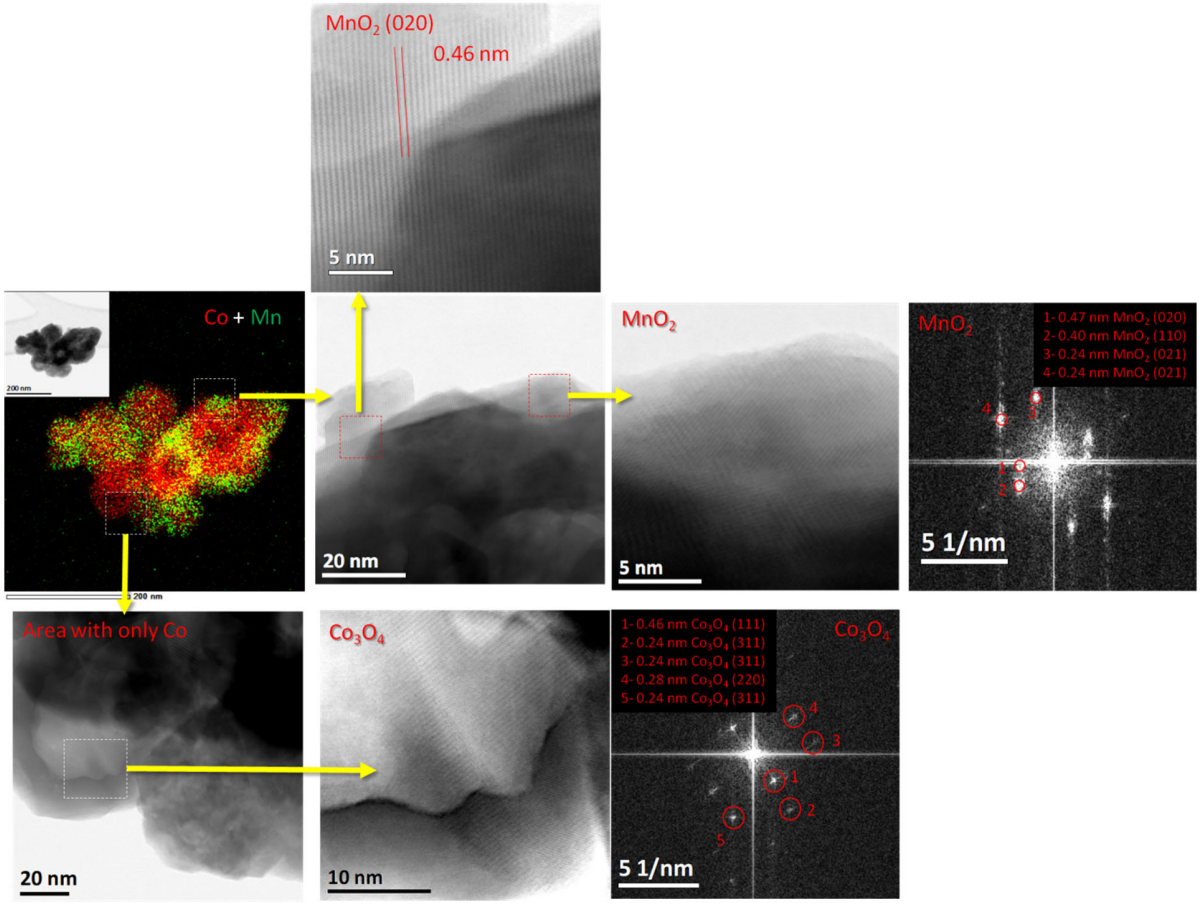

Figure S 11. STEM-EDX (middle left) image of the spent Co_8MnO_x catalyst and high resolution bright field STEM images derived from catalyst areas composed *exclusively by Co or Mn*. The interplanar spacing is indicated by two parallel lines. The squares indicate the part of the low magnification image from which the high-resolution images are derived. The FFT diffraction patterns correspond to HRSTEM images at their left side.

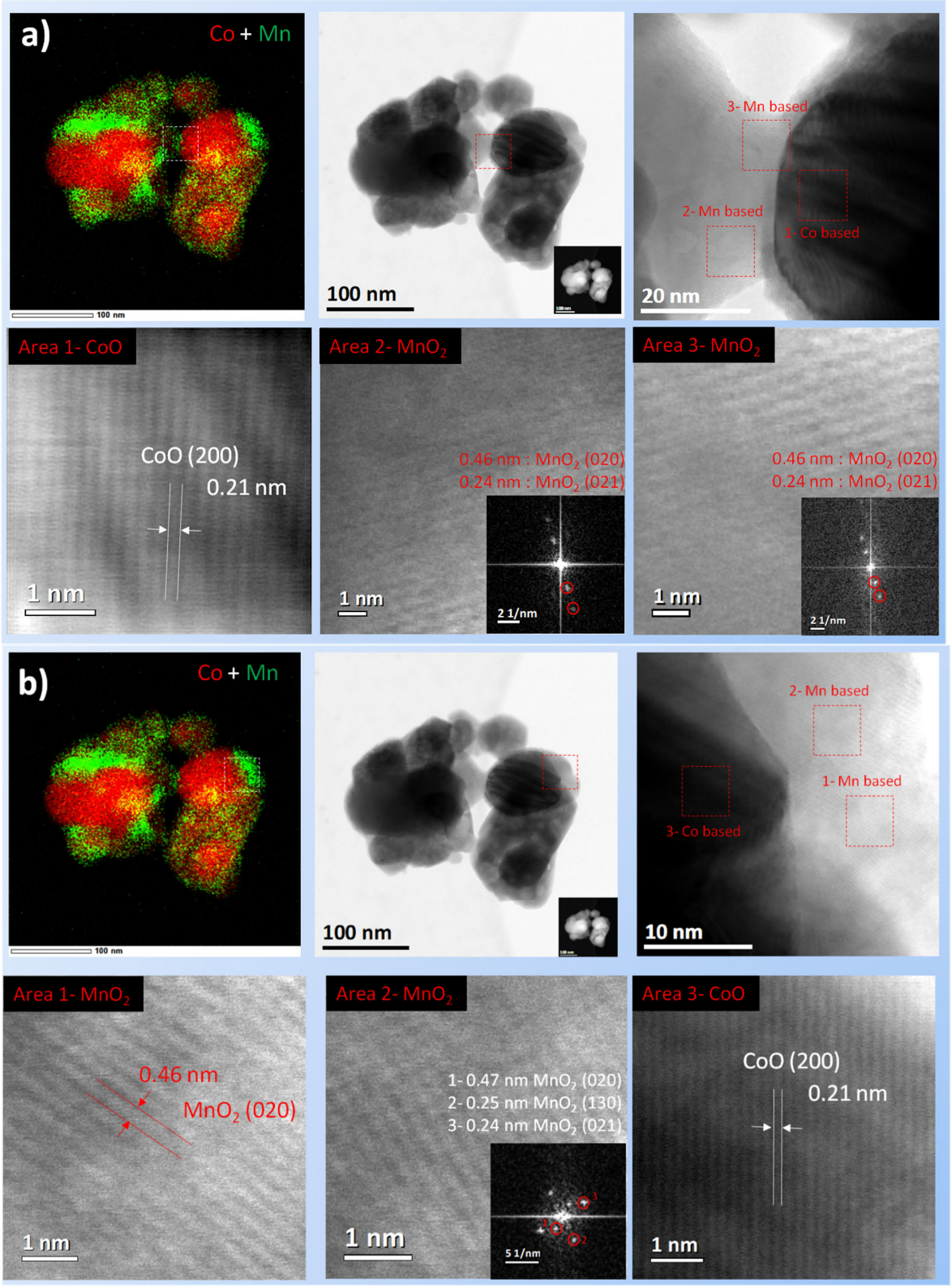
a)
Co + Mn
100 nm
100 nm
3- Mn based
2- Mn based
1- Co based
20 nm
Area 1- CoO
CoO (200)
0.21 nm
1 nm
Area 2- MnO2
0.46 nm : MnO2 (020)
0.24 nm : MnO2 (021)
1 nm
2 1/nm
Area 3- MnO2
0.46 nm : MnO2 (020)
0.24 nm : MnO2 (021)
1 nm
2 1/nm
b)
Co + Mn
100 nm
100 nm
2- Mn based
1- Mn based
3- Co based
10 nm
Area 1- MnO2
0.46 nm
MnO2 (020)
1 nm
Area 2- MnO2
1- 0.47 nm MnO2 (020)
2- 0.25 nm MnO2 (130)
3- 0.24 nm MnO2 (021)
1 nm
5 1/nm
Area 3- CoO
CoO (200)
0.21 nm
1 nm

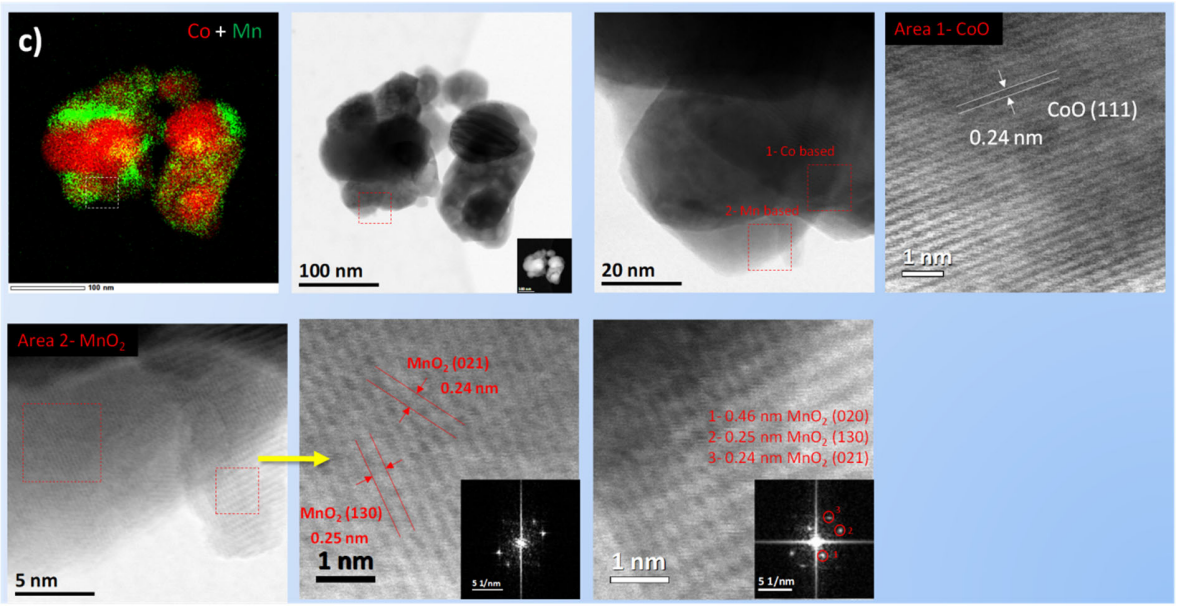

Figure S 12. STEM-EDX (top left) image of the spent Co_8MnO_x catalyst and the high resolution bright field STEM images derived from 3 individual areas (a, b, c) of the same aggregate where *Co and Mn overlap*. The interplanar spacing is indicated by two parallel lines. The squares indicate the part of the low magnification image from which the high-resolution images are derived. The FFT diffraction patterns are included in several images.

Supporting information 12: Comparison of Co 2p peaks

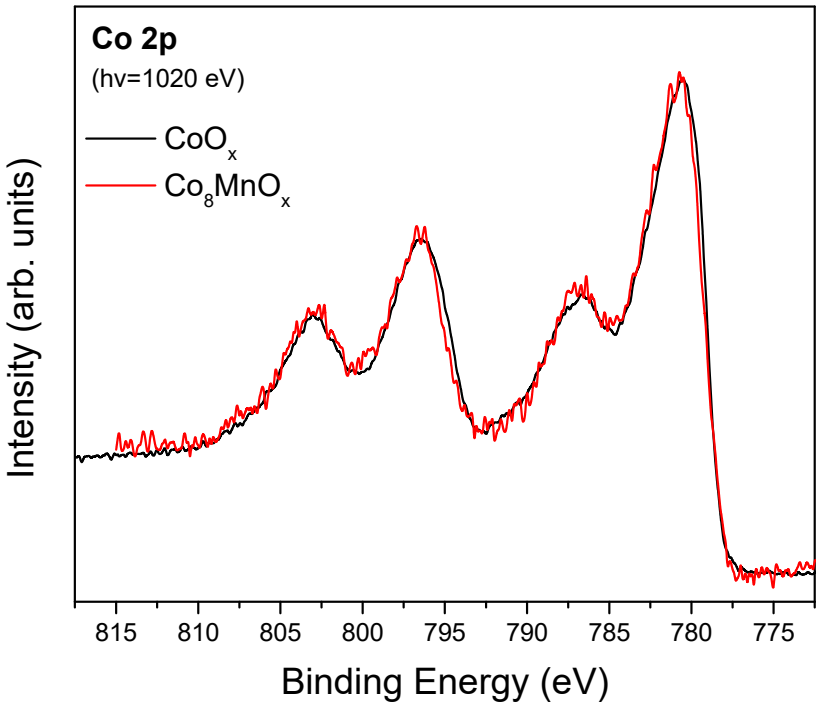

Figure S 13. Comparison of NAP-XPS Co 2p spectra recorded over CoO_x and Co_8MnO_x catalysts (hv=1020 eV) under conditions where CoO is dominant. The almost identical peak profiles do not support the possibility of a mixed Co-Mn phase formation over Co_8MnO_x catalysts.

Supporting information 13: SESSA quantitative simulations of XPS peaks

SESSA simulations

The SESSA simulations of the Co 2p and Mn 2p peak intensities were performed for surface arrangements consisting of MnO_2 particles supported on planar CoO substrate (see Figure S15). Three different MnO_2 particle morphologies were modeled in the calculations i) cubic ii) hemispheres and iii) regular pyramids with square base. The calculations were performed for 5 different particle heights (thicknesses): 1.5 nm, 3 nm, 6 nm, 50 nm, 500 nm, which were kept identical for every particle shape. In the simulations the density of the particles on the support was left to vary up to the point that the calculated Co 2p and Mn 2p peak area ratio converge with the experimental one. Practically, the particles density was defined by "X-Y period" of the particles as a function of the area at the base of the particle i.e. "X-Y length". The total surface area was the sum of the surface of the MnO_2 particle(s) (calculated every time by a different formula according to the particle shape) and the planar support (always a square, found by the X-Y period), minus the area at the base of the particle (evidently this part is not accessible to the BET surface area measurements). The % CoO surface was found by subtraction of the MnO_2 surface area from the total one. The calculated values are given in Table S3.

Figure S 14. Characteristic screenshots of the SESSA software related to the experimental setting, model and calculation windows.

As shown in Table S3 the %CoO surface area was increasing with the particle size, independently of the morphology of the particle, however the absolute value of %CoO depends on the morphology. In order to narrow the uncertainly of the calculation we also calculated the %wt of Mn in the catalyst, using the densities of MnO_2 and CoO (in this case we calculated the volumes of the particle and the substrate respecting their dimensions). The %CoO value that satisfies both the experimental Co2p/Mn 2p intensity ratio and the nominal loading of Mn on Co (ca. 12%wt. Mn) was in average around 24% CoO area and it was very similar for all sample shapes. This value (24%) was used as the estimation of the uncovered cobalt areas on the Co_8MnO_x in order to calculate the effective surface area of this catalyst.

Table S3. SESSA simulations

Hemispheres	**Thickness (Å)**	**Radius (Å)**	**X-Y Period (Å)**	**Mn/(Co+Mn)**	**%Co surface area**	**Mn %wt**
	15	15	35	19.82	26,8	11,4
	30	30	85	19.69	43,8	6,7
	60	60	190	19.57	52,3	4,9
	5000	5000	16500	19.89	55,2	4,4
Cubic particles	**Thickness (Å)**	**X-Y length (Å)**	**X-Y Period (Å)**	**Mn/(Co+Mn)**	**%Co surface area**	**Mn %wt**
	15	15	23	20.40	18,4	17,8
	30	30	55	19.37	28,2	11,2
	60	60	118	19.79	32,3	9,3
	500	500	1030	19.65	35,1	8,2
	5000	5000	10400	19.41	35,7	7,9
Pyramids with square base	**Thickness (Å)**	**X-Y length (Å)**	**X-Y Period (Å)**	**Mn/(Co+Mn)**	**%Co surface area**	**Mn %wt**
	15	15	15	19.97	0,0	22,5
	30	30	38	19.63	15,7	12,5
	60	60	90	19.65	27,9	7,9
	500	500	910	19.66	41,7	4,6
	5000	5000	9300	19.81	43,2	4,3